



ORIGINAL ARTICLE

Calculation of the load-bearing capacity of a wood-wood joining system adapted to digital and democratized manufacturing

Antonio Jesús de-los-Aires-Solís^{a,*}, Jesús Cuadrado Rojo^b

^aDoctoral School, University of the Basque Country, UPV/EHU, 48940 Leioa (Bizkaia), Spain

^bDepartment of Mechanical Engineering, University of the Basque Country, UPV/EHU, 48940 Leioa (Bizkaia), Spain

*Corresponding Author: Antonio Jesús de-los-Aires-Solís. Email: adelosaires001@ikasle.ehu.eus

Abstract: CAD/CAM technology applied to wooden structures means that traditional joining techniques, rather than metal-fastener-based systems, can now be industrialized. The development of the "Spatial Masterkey" system manufactured with a 3-axis CNC milling machine is presented. The system democratizes traditional joining techniques. It is designed for the construction of lightweight roofs, based on articulated joints with 50x50 mm section bars, working under traction and compression. A test campaign involving 6 different trials was proposed for the evaluation of the behavior of the different nodes. Satisfactory practical results were obtained in relation to the estimated theoretical values. Tensile and compressive tests on the horizontal/vertical bar nodes yielded higher results than the calculated values (8.50 kN before failure). With regard to the tests on the diagonal bars, cylindrical doweling reinforcements were required, which increased the resistance capacity by almost 130%. Future lines of research that can be pursued within this field are also proposed.

Keywords: Wood-wood joinery, democratized digital manufacturing, "Spatial Masterkey", spaceframe; sustainability, physical testing

1 Introduction

Structural wooden joints are the most conflictive points in a wooden structure and are of special interest, in so far as the struts that form the structure either become discontinuous or reduce their effective section (art 5.2. [1a]) at those points, due to the milling process that is necessary to assemble the wood-to-wood joints.

Advances in digital manufacturing [2, 3] have also implied looking back at the past and reviving joinery assembly techniques [4] that, due to the use of metallic fasteners to join parts, had fallen into disuse [5-8]. Mass customization of traditional joinery techniques can now be done [9-13], thanks to CNC production tools, making their use not only highly competitive -rivaling metallic fasteners across a range of specific uses- but, above all more respectful of the environmental, through the elimination of fasteners [14-16]. The contribution of this paper is the reinterpretation of carpentry joints through digital design, using an affordable and easily accessible 3-axis CNC milling machine for the production of a new wood-wood joining system known as the "Spatial Masterkey" [17].

1.1 Background of the research and current state of research in this field



The research and development of the “Spatial Masterkey” joining system was inspired by an analysis of a 3D wooden puzzle called “Snowflake” (**Figs. 0 (a, b)**) whose formal configuration and unique method of interlocking its constituent pieces make it a system with the potential to generate complex spatial structures.

After converting the “Snowflake” puzzle to meet the requirements of digital manufacturing, so that, in addition to it becoming a structural element, its manufacture could be digitalized, and industrialized, and access to it could be democratized, it was named the “Spatial Masterkey” joining system (**Fig. 0(c)**).

The adaptation of the “Snowflake” puzzle to digital manufacturing and its configuration as a structural element meant having to modify both the shape of some pieces of the original puzzle and their joining systems. In that respect, it should be noted that the pieces that constitute the “C” shaped diagonals (orange box - **Fig. 0(b)**-) were converted into 3 independent “I” shaped bars (green box - **Fig. 0(c)**-), so as not to waste material during their manufacture (a key aspect in prefabrication). From among the 3 bars, the central one was not needed in 2/3 of cases, so the diagonal consisted of a single bar (yellow box - **Fig. 0(c)**-). In the remaining third, the independent bars had to be mechanically joined together again to reconstitute the “C”, so doweling reinforcements were inserted to strengthen the bars (red box - **Fig. 0(c)**-). It should be noted that the shape of the bars was modified in this phase of studying the joining system (strength-capacity evaluation phase), due to both the reinforcements and the perforations cut into the bars to join the aforementioned parts, as a consequence of the progressive improvements, as can be seen in the following figures. Regarding the current state of research in this field, there are other construction systems developed under the same premises (industrialized digital manufacturing and universal access) as the “Spatial Masterkey” joining system. Examples drawing on the same philosophy can be found in projects such as “WikiHouse” [53], in the “Arches” project by the Boano Prismontas architectural studio [54], in the “X-Frame” [55], “CLICK-RAFT” [56], “Wood Frame Grammar” [57], “Sim[PLY]” [58], “[SI-MODULAR]” [59] construction systems.

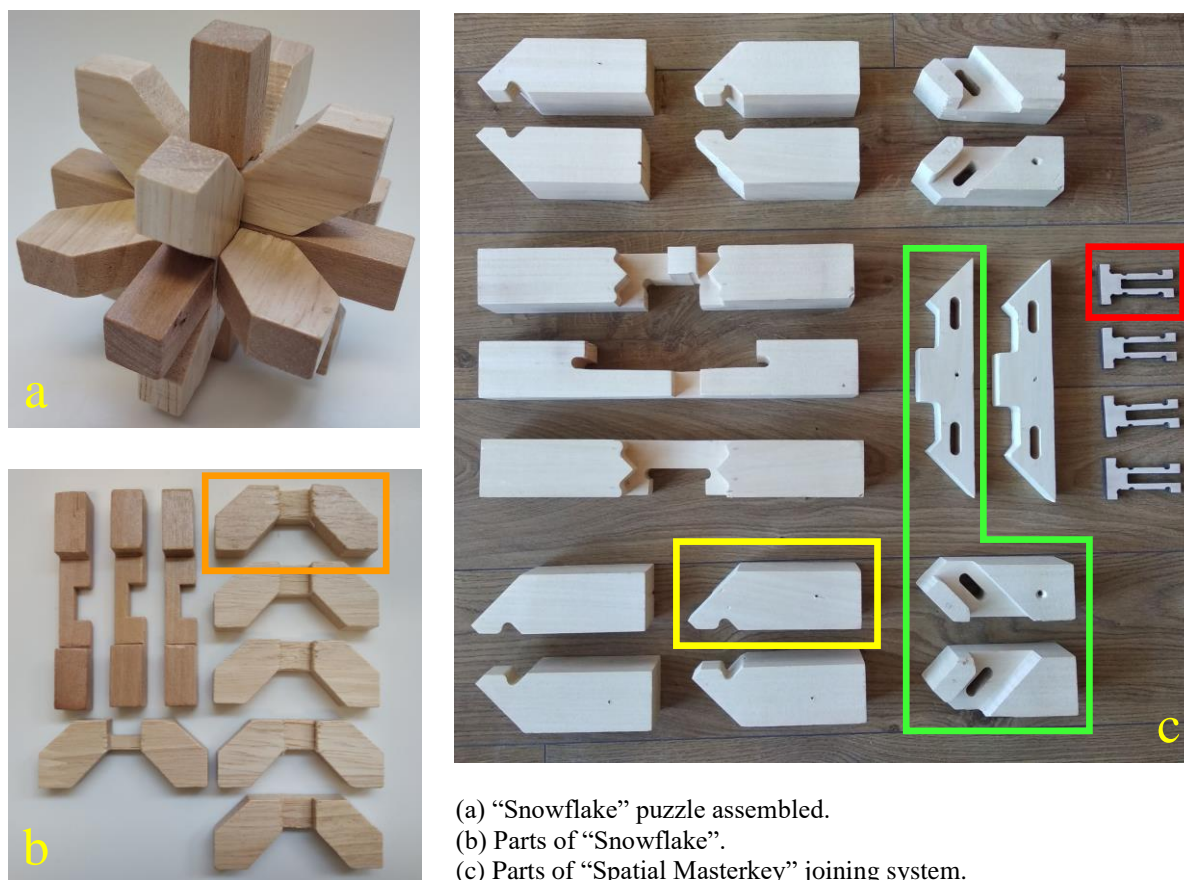


Fig. 0. “Snowflake” puzzle and “Spatial Masterkey” joining system.

2 Design of the “Spatial Masterkey” wood-wood joining system

A digital manufacturing process was followed in the design and manufacture of the “Spatial Masterkey” wood-wood joining system [17] (**Fig.1**), because of the advantages that it brings to the milling of wood-wood joints (cutting speed and precision, and dimensional uniformity) [7, 18]. The use of this joining system is not only competitive, but also respectful of the environment, because the joints that are made of wood have a very low carbon footprint. The raw material from which the joints are processed has emitted no green-house gases during its growth and requires little energy during its production process. Moreover, wood products can be considered a carbon sink, as they have negative CO₂ emission coefficients [19]. Compared to conventional building materials, they are the most environmentally friendly [20-21].

A Computerized Numerical Control (CNC) 3-axis milling machine was chosen for the manufacture of the “Spatial Masterkey” system with the sole aim of “democratizing” the production of the joints [2, 22-23] and, therefore, the structures that can be manufactured with them. An affordable tool is employed that is easily accessible in society, both because of its low cost, if its purchase is desired, and because of the ease with which a single person can manufacture products using economic components. Nevertheless, that advantage may have implied a limitation when designing the geometry of the “Spatial Masterkey” as a consequence of the specific restrictions of the CNC machine, in so far as the milling head only functions with the workpiece positioned on a normal flat surface, and can only move the cutter along three axes: X, Y, and Z.

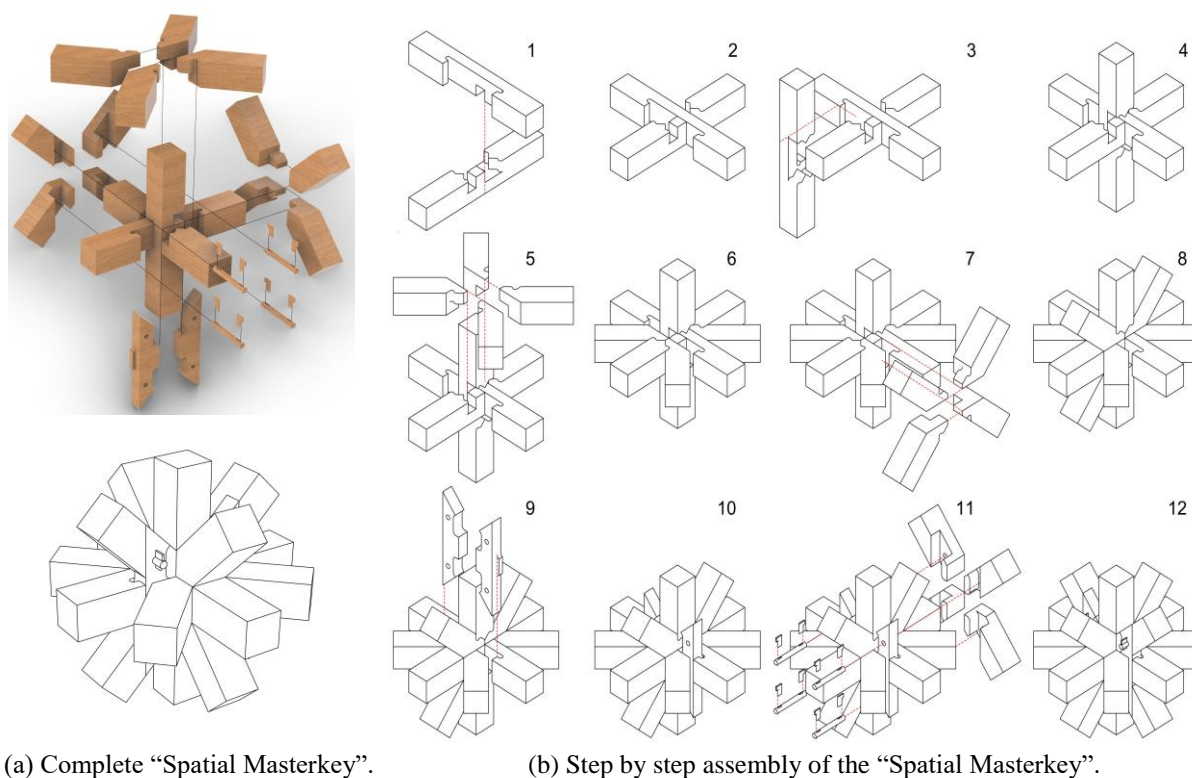


Fig. 1. “Spatial Masterkey” wood-wood joining system.

The “Spatial Masterkey” wood-wood joining system not only comprises a “complete” set of node connectors, but also the adaptations (**Fig. 19**) that are necessary to resolve the joints of the spaceframe when the number and the position of the struts that are joined within each set of node connectors vary -on most occasions, the “complete” set of node connectors is not needed-. The removal of struts implies altering the balance of the initial set of node connectors, which leads to specific adaptations of some of them to guarantee the integrity of the structural joints. The “Spaceframe Module” (**Fig. 20**) represents the set of spatial connectors, selected to determine the adaptations of the “complete” set of connectors.

3 Strength class and properties of the wood

Sawn *Pinus sylvestris*, was used for the manufacture of the “Spatial Masterkey” joining system and related tests.

A method was applied for the determination of the mechanical properties of this sort of wood that assigns a strength class to the wood, on the basis of certain quality parameters -for which purpose the singular aspects (knots, splits, grain irregularities, *etc.*) were analyzed in a representative joint of wooden pieces- associated with a series of strength, rigidity, and density values. That categorization is needed to define the mechanical properties of the wood that will be used as a structural component.

The method in question was the “visual classification of wood”, covered in the Spanish norm UNE 56544:2022 [24], which specifies three visual qualities of sawn coniferous wood for structural purposes (ME-1, ME-2 and MEG). The wooden workpieces met the visual quality criteria class ME-1.

A C27 strength class was assigned to the quality rating -ME-1- of the *Pinus sylvestris* species (Annex C, Table C.1 [1b]); the strength, rigidity and density values associated with this class of sawn wood are presented in Annex E, Table E.1 of the Código Técnico de la Edificación Seguridad Estructural- Madera [Technical Building Code Structural Security - Wood] [1c].

This quality-based classification norm guarantees that the values of the sawn-wood properties classified in that way will be equal or greater than the corresponding values of the assigned strength class.

4 Criteria considered to evaluate the stress/strain levels of the node connectors that form the “Spatial Masterkey” wood-wood joining system

When modeling the possible structures for which the Spatial Masterkey joining system could be developed, it was understood that the forces acting upon them would be applied to the set of node connectors. In addition, the necessary tolerances to be taken into account, so that the machined pieces interlock with each other, favors the independent movement of the struts and avoids any possible transfer of moments due to low rotational stiffness [25-28]. It may therefore be concluded, in the view of the above, that the joints behave as articulated joints.

The evaluation of the stresses to which the struts that form the joints may be subjected were conducted through experimental tests on two axial strain types -traction and compression- in view of what was indicated earlier -which is to say, due to the inappreciable effect of moment-related stress levels.

5 Evaluation of the load-bearing capacity of the “Spatial Masterkey” joining system through experimental methods

5.1 Experimental method

The experimental method consisted in subjecting the real material -which is to say, the struts that will be assembled to form the spatial structure- to a series of tests. That type of method yields high quality results, because the evaluation is conducted on a 1:1 scale prototype that accurately represents the physical and constructive features and the real stress state of the struts that will be used when assembling the structure [29].

There is a wide range of scientific literature regarding the analysis of the behavior of wood-wood joint systems subjected to different types of stresses through laboratory tests. This is due to the importance of understanding the failure modes of the joints that constitute wood-wood structures prior to their installation:

- Either, in order to improve their design, by means of an iterative design-manufacturing-testing process, in order to propose solutions, that prevent structural collapse.
- Or to understand the limits and range of use in which wood-wood joint systems can be applied.

Most publications focus on mortise and tenon joints [30-33], dovetail joints [34-40], scarf/splice joints [39-43], and step joints [44-46], as these systems are frequently used in a large number of connections in traditional building structures.

In view of Section 4, on the transfer of moments in the structure assembled with this joining system and to simplify the laboratory tests, solely axial traction and compression strain levels will be estimated in the struts that form the joints. In that way, the load-bearing capacity of the “Spatial Masterkey” joining system may be evaluated with experimental methods.

5.1.1 Manufacture of the parts of the “complete” node of the “Spatial Masterkey” joining system to evaluate its load-bearing capacity in laboratory tests

The parts of the “complete” node of the “Spatial Masterkey” joining system, necessary for the viability of the axial (traction and compression) tests in the relevant universal testing machines, were machined for the laboratory tests, without it implying any negative effects on the reliability of the results, had they been compared to the test results on the “complete” set of node connectors. In other words, precise and essential load-bearing conditions were reproduced in the assembled struts, so that the physical traction tests on the 3 types of struts -on one of the horizontal/vertical node connectors, on the single piece diagonal node connectors, and on the two-piece node connectors- were both under traction (shown in **Fig. 3, 5, and 7**), and under compression (shown in **Fig. 4, 6, and 7**)- on the same types of struts, so that the results could be as close to the real structural behavior of the complete set of spatial node connectors. The above amounts to a total of 6 test set-ups (**Fig. 2**).

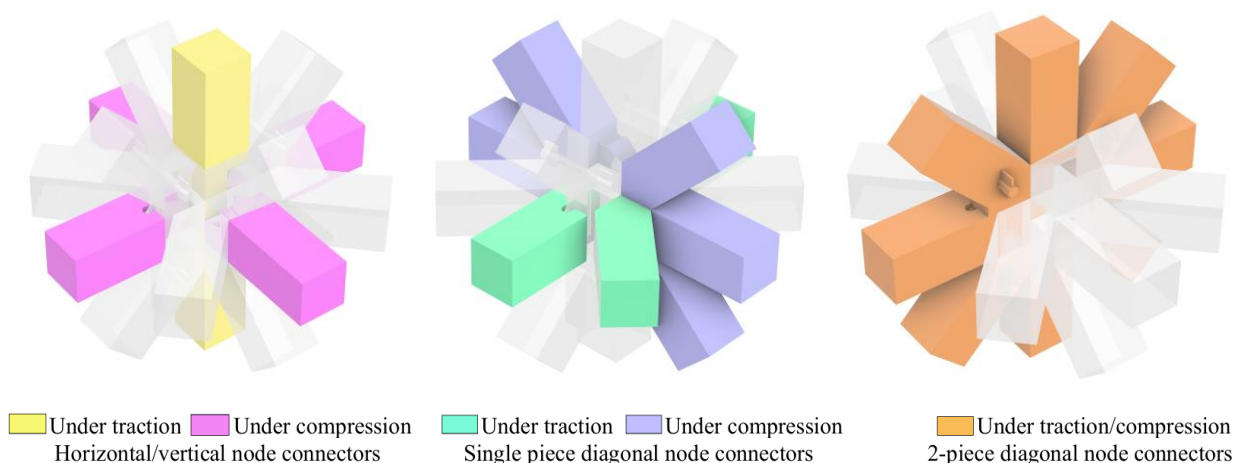


Fig. 2. Parts of the “complete” node of the “Spatial Masterkey” joining system necessary for axial strength tests.

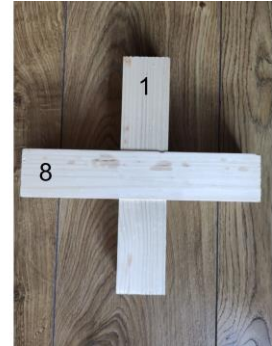
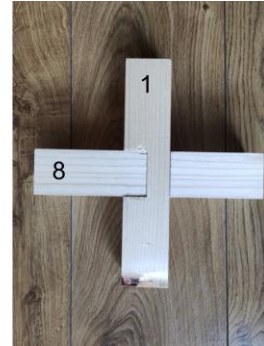
The maximum number of pieces to manufacture and, therefore, the composition of the node connectors to evaluate the load-bearing strength of the 3 types of struts, differed between the traction and the compression tests in the analyses of both the horizontal/vertical node connectors (**Fig. 3 and 4**) and the single diagonal piece (**Fig. 5 and 6**).

- In the first of the three cases -the horizontal/vertical node connectors- all that is necessary is the presence of 1 strut for traction tests, as its stress state is unaffected by the presence of other struts connected to the node, so that one is sufficient; whereas two pieces are needed for the compression test. The application of compressive force on the vertical strut will influence its mid-length joint with the other horizontal strut, because the presence of the latter part enlarges the effective section withstanding that force -specifically, the totality of the section of the piece- when the vertical piece is compressed.
- And in the second case -the single diagonal piece-, the composition of the struts for a proper traction test implied modifying, with regard to the compression test, the stereotomy of the joint between the single diagonal piece and the horizontal/vertical one with which it is assembled. It was done so that the joint could not “detach” after the application of traction force leading to relative displacement between one strut and the other. In addition, the strut that reproduced the horizontal/vertical node connector was milled in such a way as to ensure the viability of the traction test, so that its grain was at an angle of 45 °with the single diagonal piece, to simulate its actual placement at 45 °to the aforementioned diagonal piece. In the traction test, two struts were used (a single diagonal piece and another horizontal/vertical one). Apart from the horizontal node connector with which the single diagonal piece interlocks, in order to perform the compression test effectively on that single piece, another symmetrical single diagonal piece was needed -assembled in the same way with the horizontal strut- so as to the compressive force properly -to the axis formed by both diagonals- and another vertical strut, assembled mid-length perpendicular to the horizontal, so as to avoid any rotation of the diagonal parts that

might detach the joint. So, 4 pieces were needed for that test (two single diagonal pieces and two horizontal/vertical ones).

In contrast, in the type of 2-piece diagonal strut, the composition of the node for its traction test was identical to the one for the compression test. The configuration of the node was similar to the configuration for the compression test on the single diagonal piece and for the same reasons, with the exception that the two pieces that formed the diagonal were linked by a dowel pin. Any relative movement between both pieces in a perpendicular direction to the plane when the loads were applied was therefore prevented.

HORIZONTAL/VERTICAL NODE CONNECTORS



(a) Pieces of the node.

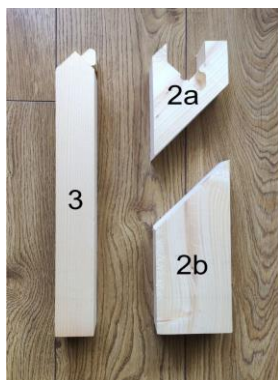
(b) Assembled (Front).

(c) Assembled (Back).

Fig. 3. Under traction.

Fig. 4. Under compression.

SINGLE PIECE DIAGONAL NODE CONNECTORS



(a) Pieces of the node.

(b) Assembly phase 1.

(c) Assembled

Fig. 5. Under traction.



(a) Pieces of the node.

(b) Assembly phase 1.

(c) Assembled (Front).

(d) Assembled (Back).

Fig. 6. Under compression.

2- PIECES OF THE DIAGONAL NODE CONNECTOR

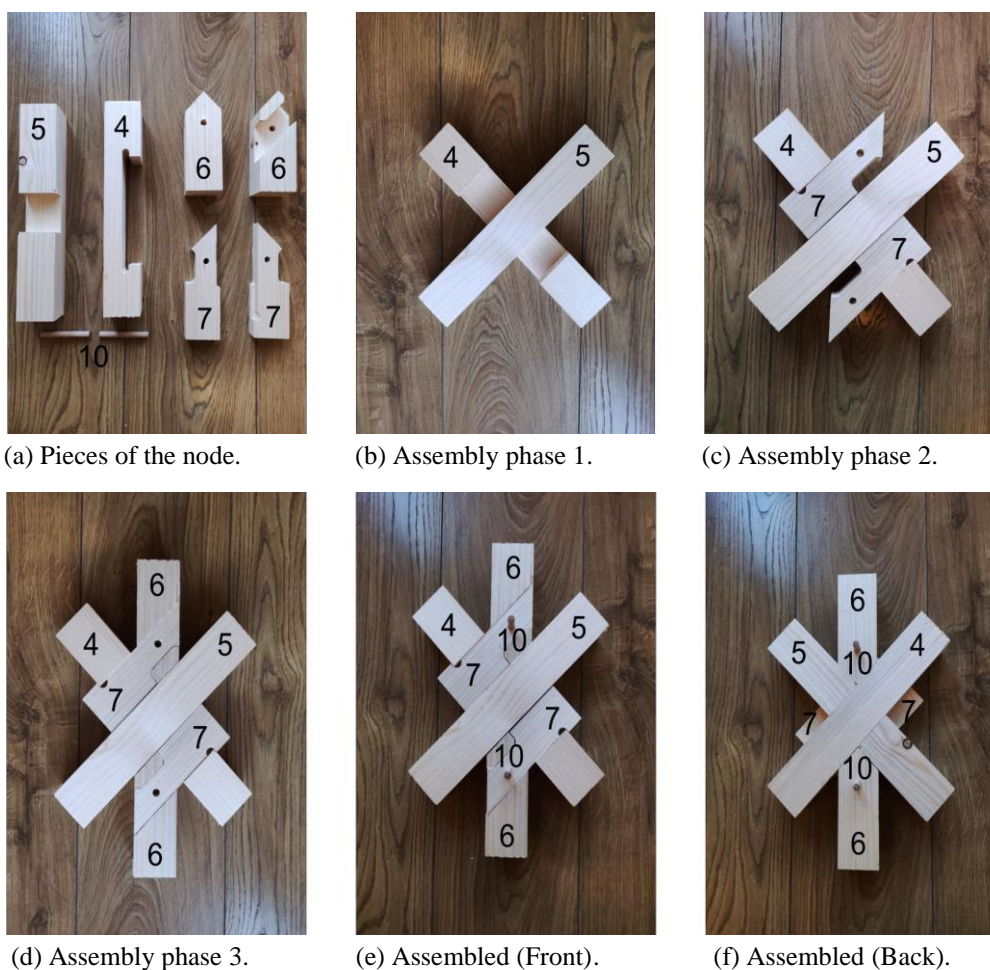


Fig. 7. Under traction/compression.

The numbers on the struts refer to those shown in **Fig. 8**.

One very important aspect to consider is the need to contemplate tolerances in the specific design of the model, in order to manage not only machining imprecision, but also possible volumetric movements of the material.

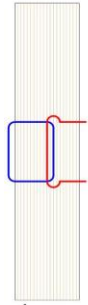
The necessary tolerances were defined in experimental terms through an iterative process during the process of milling the pieces. That parameter, introduced in the preparation of the CAM file, was continually adjusted until the milled perimeters of the pieces to be placed in contact with each other fitted together perfectly, while allowing for easy assembly and disassembly (in this case 0.4 mm in the perimeters where there is contact between the pieces).

The pieces used in this test were made of *Pinus sylvestris*, except for the dowel pins that were made of *Fagus sylvatica*.

The considerations taken into account in the design of the cut-outs of the pieces to optimize the manufacturing were as follows:

- They had to be completed in such a way that the machining of each piece was a single operation (with no need to stop the manufacturing process to reposition the pieces) and using a single, straight, 8 mm cutter. In doing so, both inaccuracies and increased milling times were avoided.
- The assembly/disassembly of the structures, piece by piece, was not prevented.

The following images depict the CAD design of the milling paths, the manufacturing process, and the product, which was machined with a 3-axis CNC machine and then assembled with the node connectors for testing (**Fig. 8**).



1



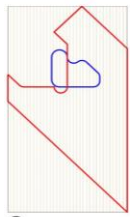
Mortising (blue path). Z: 0 to 22,5 mm



Cutting (red path). Z: full thickness



Milled piece



2a



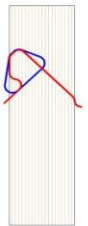
Mortising (blue path). Z: 0 to 22,5 mm



Cutting (red path). Z: full thickness



Milled piece



3



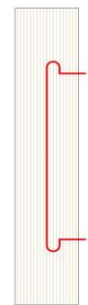
Mortising (blue path). Z: 0 to 22,5 mm



Cutting (red path). Z: full thickness



Milled piece



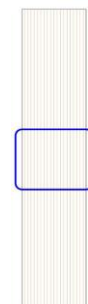
4



Cutting (red path). Z: full thickness



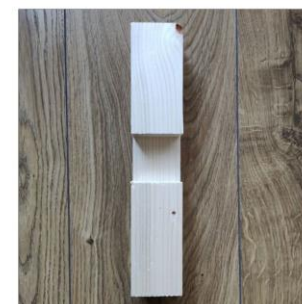
Milled piece



5



Mortising (blue path). Z: 0 to 22,5 mm



Milled piece

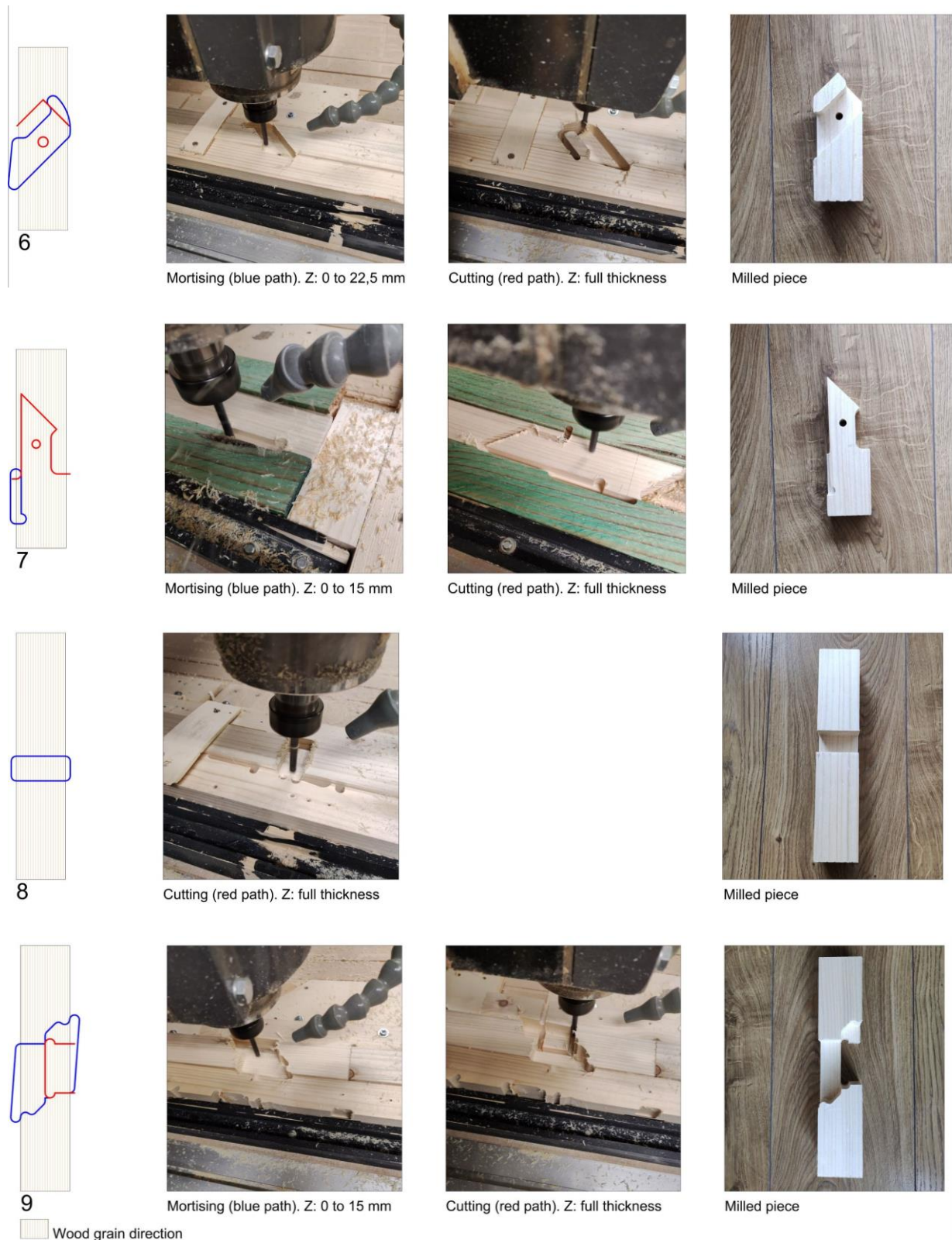


Fig. 8. Cutting path, manufacturing process, and final product assembled with the pieces milled by the CNC machine.

5.1.2. Considerations when performing the laboratory tests and their results

The load-displacement traction tests were conducted on a 100 kN “Ibertest” universal testing machine, with a precision class, as per ISO 7500-1 of 0.5, and a displacement resolution of 0.001mm.

The compression tests were conducted on a 300kN “Test Systems” universal testing machine, with

a precision class of 0.5, as per ISO 7500-1, and a displacement resolution of 0.001mm.

The parameter that was considered when conducting the test was deformation per minute of the node connectors under traction/compression subjected to that force -specifically, 0.6 mm/min-.

Given the stereotomy of the carpentry joints, in which the necessary tolerances have to be defined, so that the milled pieces of each connector can be interlocked with each other, the higher the number of node connectors, the higher the accumulation of tolerances. In consequence, greater deformations will be obtained before the collapse of the joint, whether under traction or compression.

This hypothesis will be justified in the descriptions of each test.

The aim is to determine the necessary traction/compression force to be applied to the different sorts of struts that form the “Spatial Masterkey” joining system before the nodes collapse, due to failure of some of the struts.

The tests and their results are described below for each type of strut when applying the axial loads in the direction of their longitudinal axes -in line with the grain-, and where the test failures occurred in the different sets of connectors inserted in the node.

In total, 6 tests, one under traction and another under compression for each of the three types of struts were conducted -the diagonal strut formed of only 1 piece, the strut with 2 pieces and, on one of the horizontal/vertical struts-.

The different test phases are depicted for each strut type and axial force in an image of the initial state of the machine, another in its final state after the failure, and the last one showing the deformation/failure diagram (Fig. 9(a), 10(a), 11(a) -under traction- and 12(a), 13(a), 14(a) -under compression-). That analysis is complemented by a strain-deformation diagram for each of the 6 tests (Fig. 9(b), 10(b), 11(b) -under traction- and 12(b), 13(b), 14(b) -under compression-), and the image of the piece in which the failure occurred (Fig. 9(c), 10(c), 11(c) -under traction- and 12(c), 13(c), 14(c) -under compression-).

Rothoblaas TBS MAX 8x200 (8mm in diameter by 200 mm in length) flange-head screws were screwed into the sides of the struts at parallel points in the direction of the grain on the axis where the traction forces were to be applied for the traction tests. The screws served as gripping points for the test machine to apply the traction force properly for a satisfactory test. It was confirmed that in no case was failure due to the displacement of the screws in relation to the pieces in which they were inserted.

5.1.2.1 Traction tests

HORIZONTAL/VERTICAL NODE CONNECTORS

In this test, the presence of only 1 strut is necessary, as its stress state is not affected by the presence of other node connectors.

Failure occurred under a load of 8.64 kN (Fig. 9(b)), due to shear stress in a direction parallel to the direction of the grain (art. 6.1.8 [1d]) (Fig. 9(a)) within the area of the change of section of strut 1 (Fig. 3), with a tractional deformation of the strut of 6.11 mm in the direction of the load.

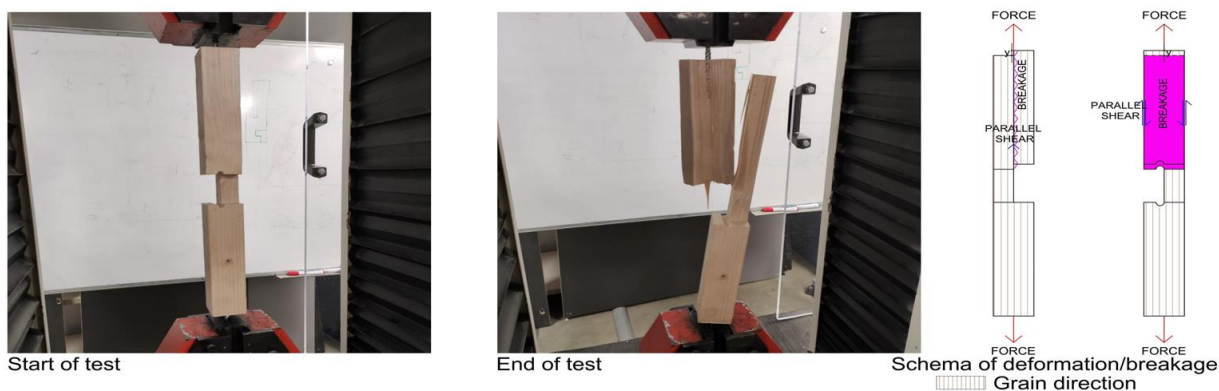


Fig. 9(a). Initial and final phase of the traction test and deformation/failure diagram of the horizontal/vertical node connector.

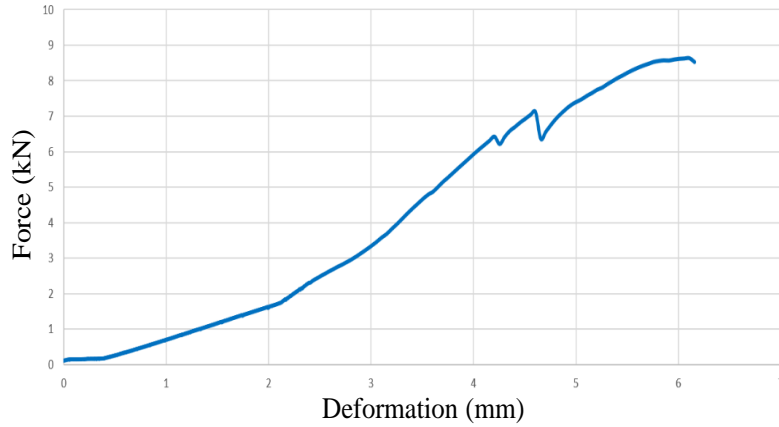


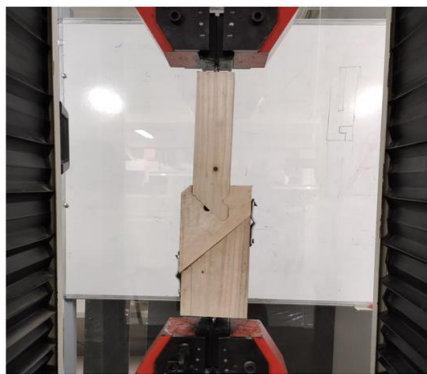
Fig. 9(b). Traction test force/deformation diagram of the horizontal/vertical node connector.



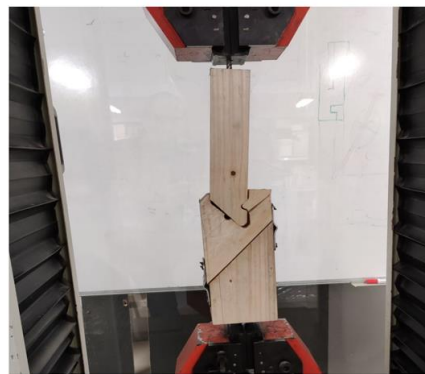
Fig. 9(c). Shear fractured piece.

SINGLE PIECE DIAGONAL NODE CONNECTORS

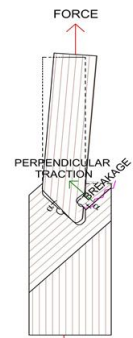
The traction applied to the struts that formed the node -diagonal strut 3 and horizontal/vertical strut 2a-b which were assembled (**Fig. 5**)- resulted in relative displacement between both that caused the failure of horizontal/vertical strut 2a-b under a load of 0.734 kN (**Fig. 10(b)**) under traction perpendicular to the grain (art. 6.1.3 [1e]) (**Fig. 10(a)**), with tractional deformation of the assembled node of 2.81 mm in the direction of the load.



Start of test



End of test



Schema of deformation/breakage

Fig. 10(a). Initial and final phase of the traction test and deformation/failure diagram of a single piece diagonal connector node

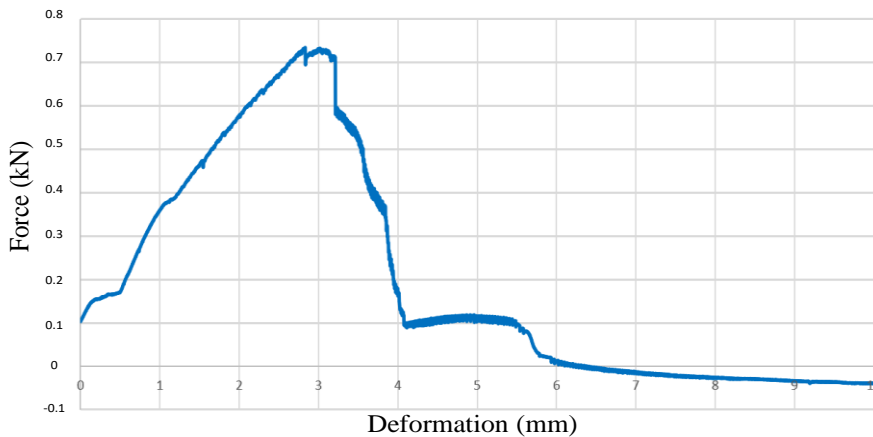


Fig. 10(b). Traction test force/deformation diagram of single piece diagonal node connectors.

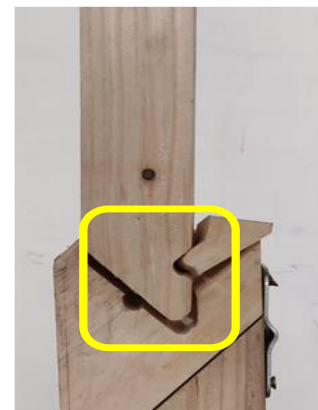


Fig. 10(c). Fractured piece under traction perpendicular to the grain.

2-PIECE DIAGONAL NODE CONNECTORS

The traction applied to the diagonal struts 6 (**Fig. 7**) caused rotation in strut 7 (**Fig. 7**) symmetrically opposite to the axis of traction and to strut 4 (**Fig. 7**); the rotation preceded the breakage of strut 4 under shear stress parallel to the direction of the grain in the assembly with one of the pieces (strut 7) as a consequence of the thrust of piece 7 upon strut 4, due to the relative rotation occurring between both (**Fig. 11(a)**).

The failure was produced under a load of 1.496 kN (**Fig. 11(b)**) due to shear stress parallel to the direction of the grain (art. 6.1.8 [1d]) in the area of interlock between strut 8 and piece 7 (**Fig. 11(a)**), with a structural deformation of 14.04 mm, due to compression in the direction of the load.

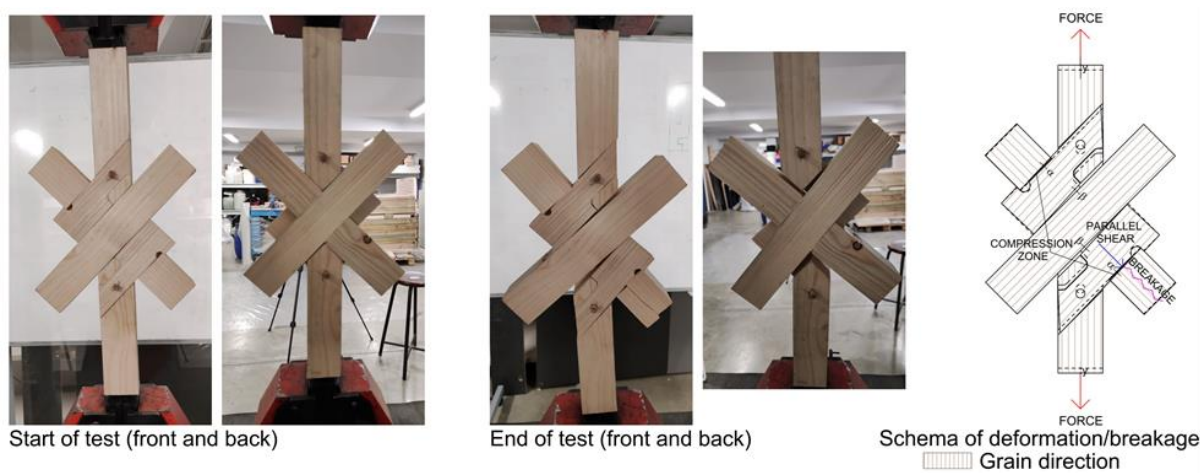


Fig. 11(a). Initial and final phase of the traction test and deformation/failure diagram of 2-piece diagonal node connectors.

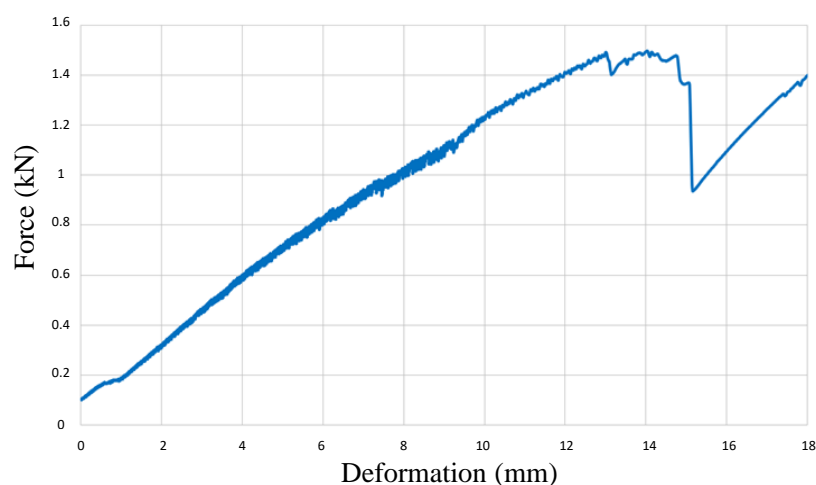


Fig. 11(b). Traction test force/deformation diagram of 2-piece diagonal node connectors.

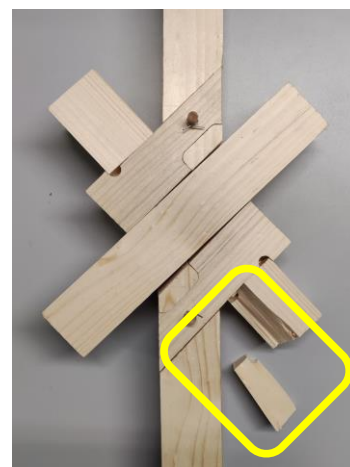


Fig. 11(c). Shear fractured piece.

5.1.2.2 Compression tests

HORIZONTAL/VERTICAL NODE CONNECTORS

The result of the compressive load applied to strut 1 (**Fig. 4**) was excentric with respect to the effective section of the strut, which caused flexion of the piece in its mid-length joint with strut 8 (**Fig. 4**), compressing the grain of the strut in a perpendicular direction.

In view of the compressive strength of strut 1 in its effective section -parallel to its grain-, the deformation of strut 8 -as a consequence of the compression- was greater than the deformation of strut 1. Therefore, as the compressive load increased, there was greater flexural deformation of strut 1 (**Fig. 12(a)**).

Once the load reached 24.27 kN (**Fig. 12(b)**), the breakage of strut 1 occurred, due to a combination of flexural forces and axial compression (art. 6.2.3 [1f]), at its mid-length joint with strut 8 in the change of section, on a parallel plane to the effective section (**Fig. 12(a)**). The structural deformation in the direction of the load was 5.20 mm.

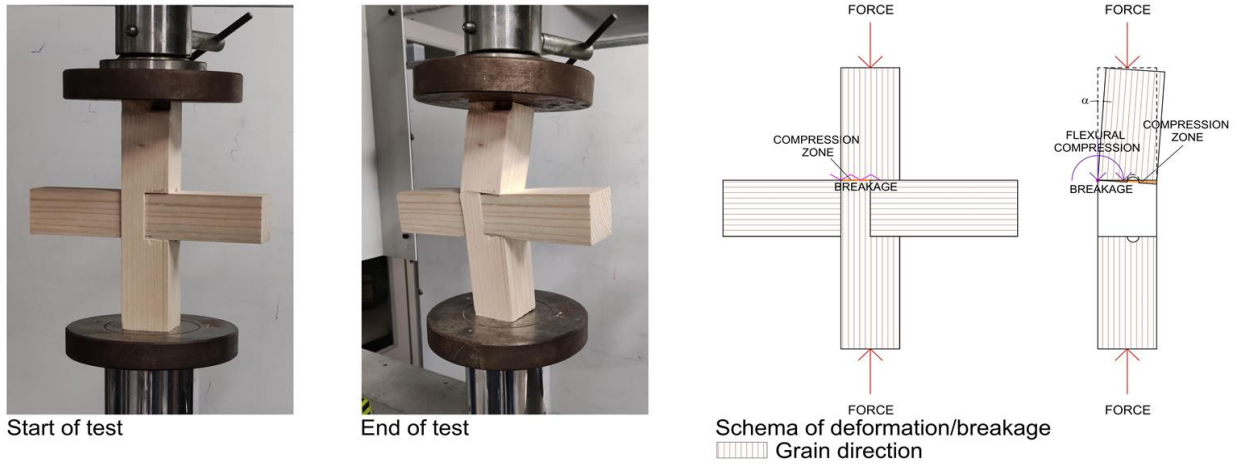


Fig. 12(a). Initial and final phase of the compression test and deformation/breakage diagram of the horizontal/vertical node connector.

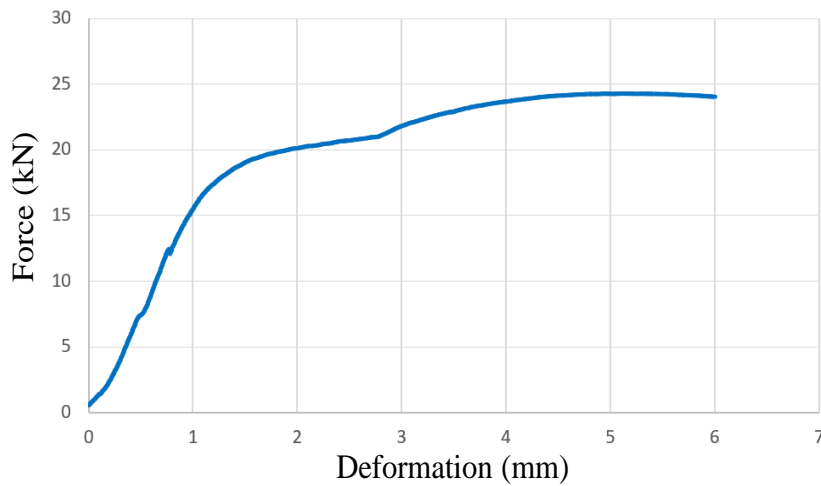


Fig. 12(b). Compression test force/deformation of the horizontal/vertical node connector.

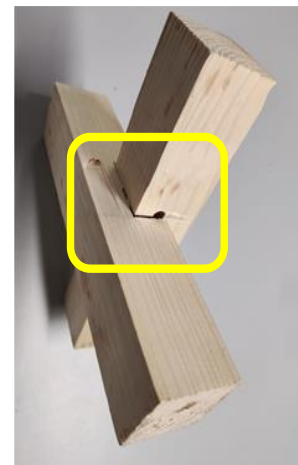


Fig. 12(c). Fractured piece under flexural compression.

SINGLE PIECE DIAGONAL NODE CONNECTORS

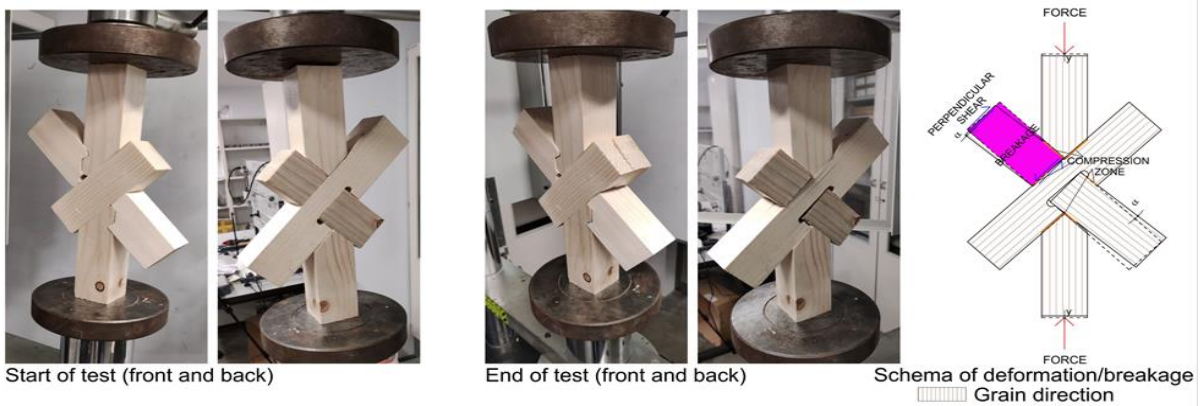


Fig. 13(a). Initial and final phase of the compression test and deformation/breakage diagram of the single piece diagonal node connectors.

The compression applied to the diagonal struts 3 (**Fig. 6**) caused them to slide in the direction of the longitudinal axis of strut 9 (**Fig. 6**), but in opposite directions; which, in addition to perpendicular compression of the grain of the aforementioned struts, provoked the rotation of strut 8 (**Fig. 6**) with respect to strut 9, which was the reason why strut 8 broke under perpendicular shear stress in the direction of the grain at the mid-length joint with strut 9. The breakage was a consequence of different strengths withstanding the rotational forces which strut 8 encountered in the aforementioned joint between the continuous and discontinuous part of strut 9 (**Fig. 13(a)**).

The failure occurred under a load of 8.00 kN (**Fig. 13(b)**), due to breakage under shear stress perpendicular to the direction of the grain (art. 6.1.8 [1d]) within the area of the change of section of the mid-length cut-out of strut 8 (**Fig. 13(a)**), with a structural deformation of 11.83 mm, due to compression in the direction of the load.

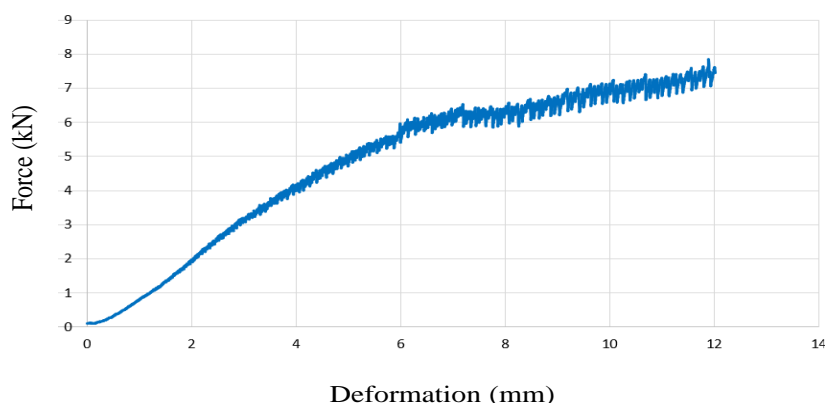


Fig. 13(b). Compression test force/deformation diagram of the single piece diagonal node connectors.

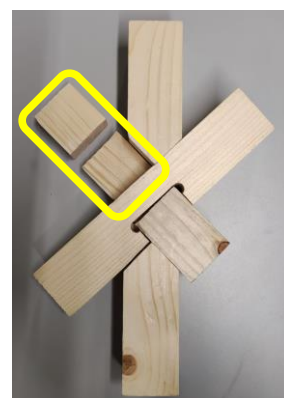


Fig. 13(c). Fractured piece under shear stress.

2-PIECE DIAGONAL NODE CONNECTORS

The interaction between each of the pieces that formed the joint in the compression test was similar to the “single piece node connector”, in so far as, for the same reasons, strut 6 (**Fig. 7**) provoked rotation in strut 5 (**Fig. 7**) with respect to strut 4 (**Fig. 7**); a rotational force that strut 5 wholly transferred to strut 7 -which formed part of the diagonal- (**Fig. 7**). The relative rotation of strut 7 compressed the end of the node connector of strut 6 -with which it was joined mid-length to form the diagonal- against strut 4. In turn, it meant that the end of strut 6 broke under parallel shear stress in the direction of the grain (art. 6.1.8 [1d]), as a consequence of the different strengths withstanding the rotation that the end of strut 6 encountered between the continuous and the discontinuous part of the aforementioned strut 4 (**Fig. 14(a)**).

The failure occurred under a load of 12.07 kN, with a structural deformation of 20.34 mm in the direction of the load (**Fig. 14(b)**).

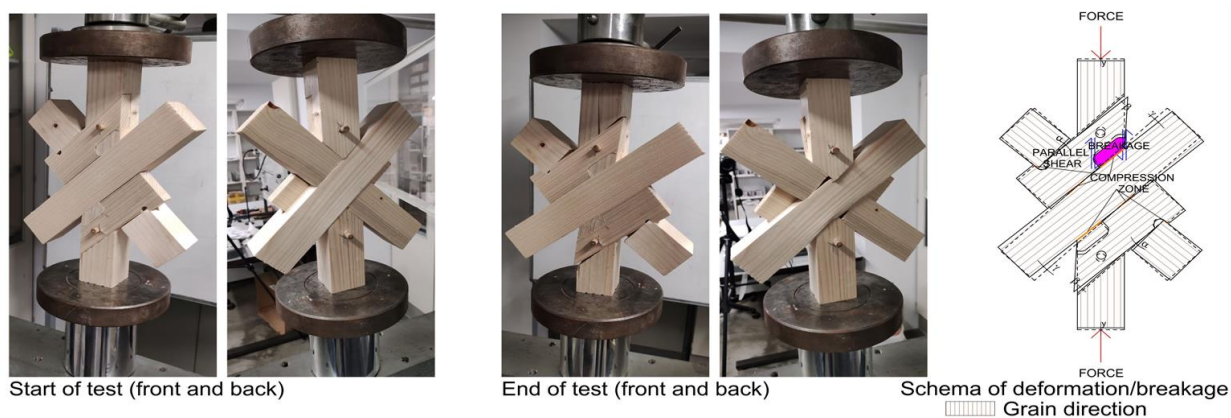


Fig. 14(a). Initial and final phase of the compression test and deformation/breakage diagram of 2-piece diagonal node connectors.

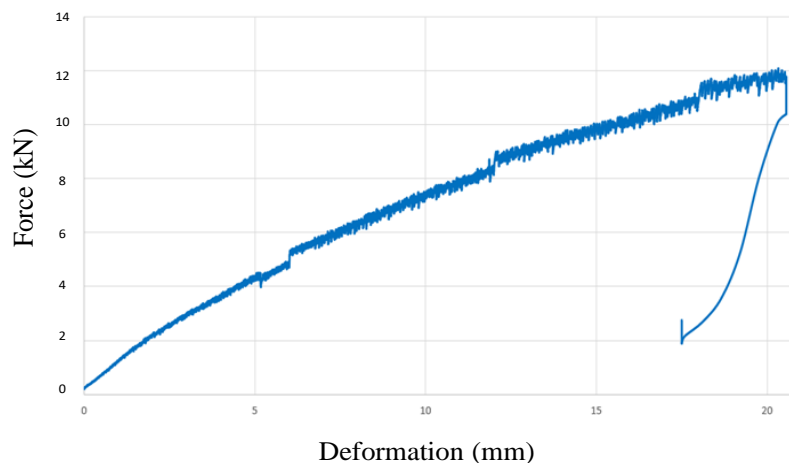


Fig. 14(b). Compression test force/deformation diagram of 2-piece diagonal node connectors.

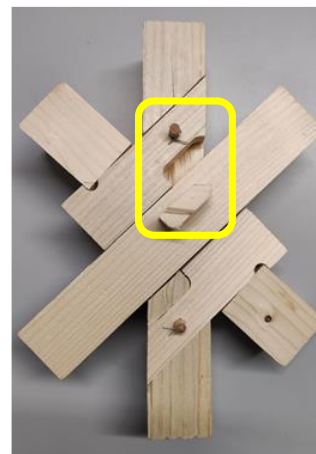


Fig. 14(c). Fractured piece under shear stress.

5.1.3 Reinforcement of the node connectors to improve their strength performance under axial stress.

In the tests, the failure of the test specimens, among which the struts that were tested under traction/compression, was not caused by breakage at the point of the least effective section of each strut as a consequence of the aforementioned stress forces. Instead, the failure occurred due to shear stress parallel to the grain or perpendicular traction in the direction of the grain (except in the compression test of the “horizontal/vertical node connectors” that was produced by compression combined with flexion -flexural compression-).

In that respect and considering that the direction of the grains in the struts was parallel to their largest -longitudinal- dimension, there were cases where the stereotomy of the joint, under traction/compression forces applied parallel to the grain of the strut that was tested, meant that the strut broke earlier under shear stress parallel to the grain, or that one strut caused the breakage of others with which it interacted, either under shear stress parallel to the grain or under traction perpendicular to the grain.

This situation is due to the characteristic strength of the sawn wooden struts under parallel traction/compression (Annex E, Table E1, strength class C27 [1c]) $-f_{t,0,k}/f_{c,0,k}-$ that is $16 \text{ N/mm}^2 / 22 \text{ N/mm}^2$, respectively; 4/5.5 times greater than the characteristic shear strength $-f_{v,k}- 4 \text{ N/mm}^2$ and 40/55 times greater than the characteristic strength under perpendicular traction $-f_{t,90,k}- 0.4 \text{ N/mm}^2$. At all times, provided that the effective section under parallel shear/perpendicular traction remains below 4/40 times that of the section under parallel traction, and below 5/55 times that of the section under parallel compression, both applied to the tests conducted on the three types of struts.

The breakage under shear stress could be avoided or, at least, could occur under a heavier load, if the struts whose breakage occurred due to the aforementioned stress levels, had formed part of a real structure with struts of greater length and, in consequence, a larger effective and therefore stronger section that could better withstand shear failure.

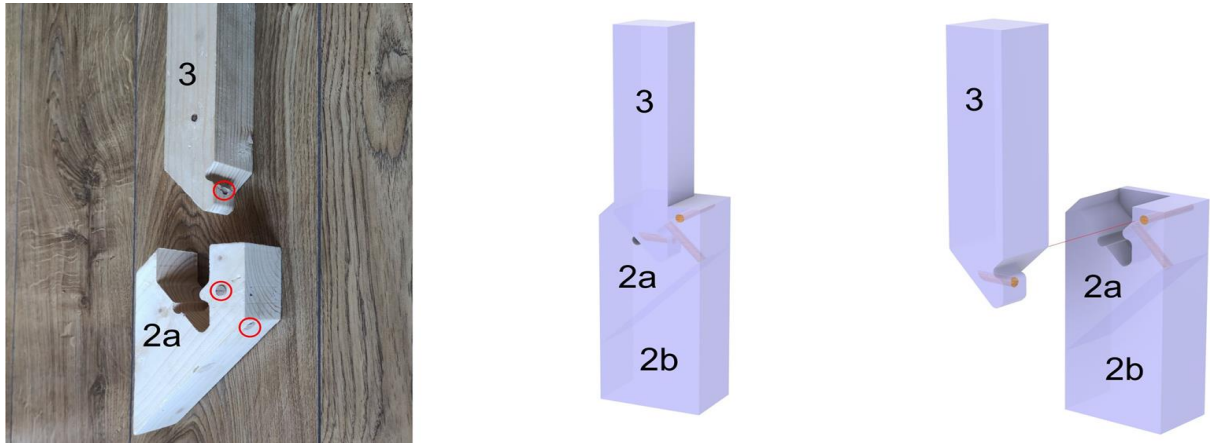
In the specific case of the tests that were performed, avoiding breakage either under parallel shear stress or under traction perpendicular to the grain, or ensuring that the failure under both stress forces took place under a higher axial force, can be achieved by inserting cylindrical wooden beechwood dowel pins of 8 mm in diameter, stuck with a polymeric wood glue with a maximum joining strength of 4,000 psi (27,579 N/mm²) as per ASTM D-905.

REINFORCEMENT OF THE SINGLE PIECE NODE CONNECTOR TO IMPROVE ITS STRENGTH PERFORMANCE UNDER TRACTIONAL AXIAL STRESS PARALLEL TO THE GRAIN.

The hypothesis that dowel pins could improve the load-bearing strength was verified in one of the tests, specifically, the traction test on the single piece diagonal node connector, because it had failed

under tractional axial stress perpendicular to the grain.

The dowel pins were inserted perpendicularly to the possible planes of parallel shear stress (in pieces 2a and 3) and traction perpendicular to the grain (in piece 3) at the points marked out below in the following images (Fig. 15).



(a) Pieces reinforced with dowel pins. (b) View of the assembled node. (c) View of the dismantled node.

Fig. 15. Reinforcement with dowel pins in the “single piece diagonal node connectors”.

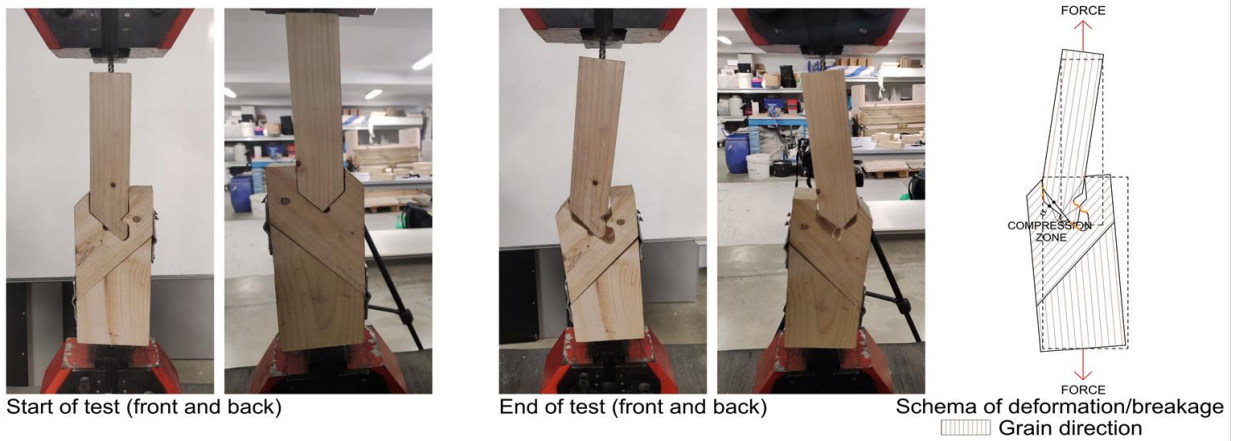


Fig. 16(a). Initial and final phase of the traction test and deformation/breakage diagram of the single piece diagonal node connector with reinforcement.

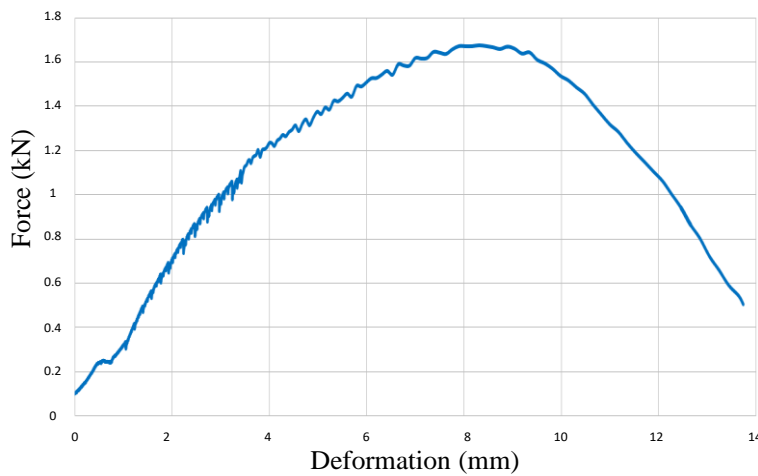


Fig. 16(b). Traction test force/deformation diagram of the single piece diagonal node connector with reinforcement

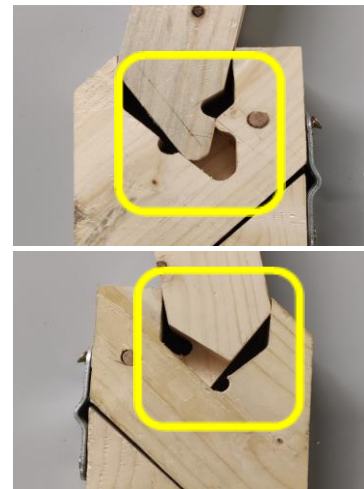


Fig. 16(c). Detached piece under traction

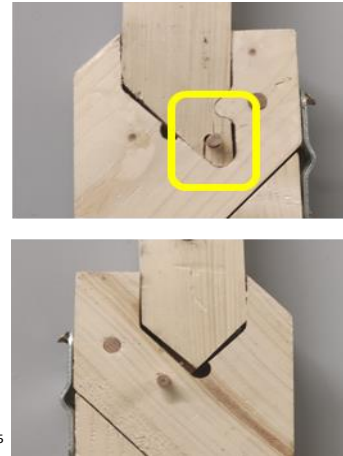
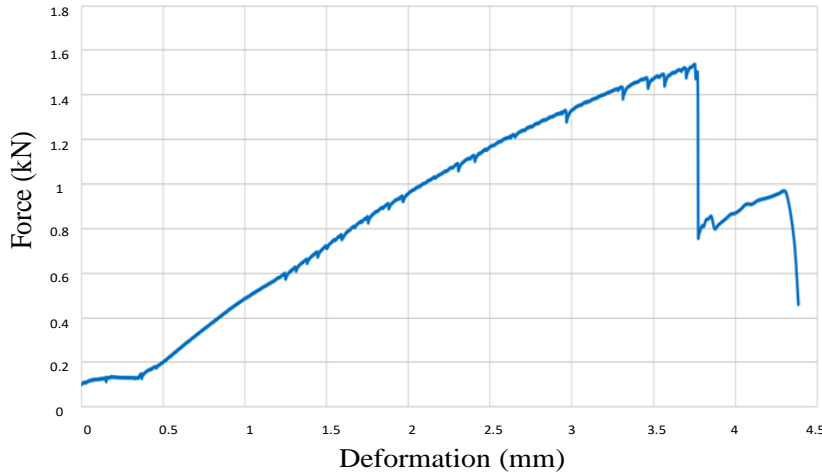


Fig. 18(b). Traction test force/deformation diagram of the single piece diagonal node connector with reinforcement+dowel pin joining pieces.

Fig. 18(c). Fractured piece under traction.

Both tests clearly showed that the reinforcement of the single piece diagonal node connectors with dowel pins to prevent collapse, either under traction perpendicular to the grain or under shear stress, considerably improved their strength performance when withstanding tractional axial stress parallel to the grain, modifying the failure mode (by 128% in the most favorable case, in which the failure of the node connectors was not due to their breakage, but due to their detachment).

In so far as this hypothesis -that the reinforcement of the node connectors to prevent undesired breakage due to low characteristic strengths could notably increase the traction force needed for node collapse- was demonstrated, and given the similarity of the stereotomy of this joint with the 2-piece diagonal node connectors under traction, the aforementioned hypothesis could be extended to those node connectors. Nevertheless, the improvement of their strength performance was not quantitatively evaluated.

6 Spatial module: type of active vector structure selected for evaluating the stress/strain exerted on the struts that form the “Spatial Masterkey” joining system

6.1 Description of the spatial module

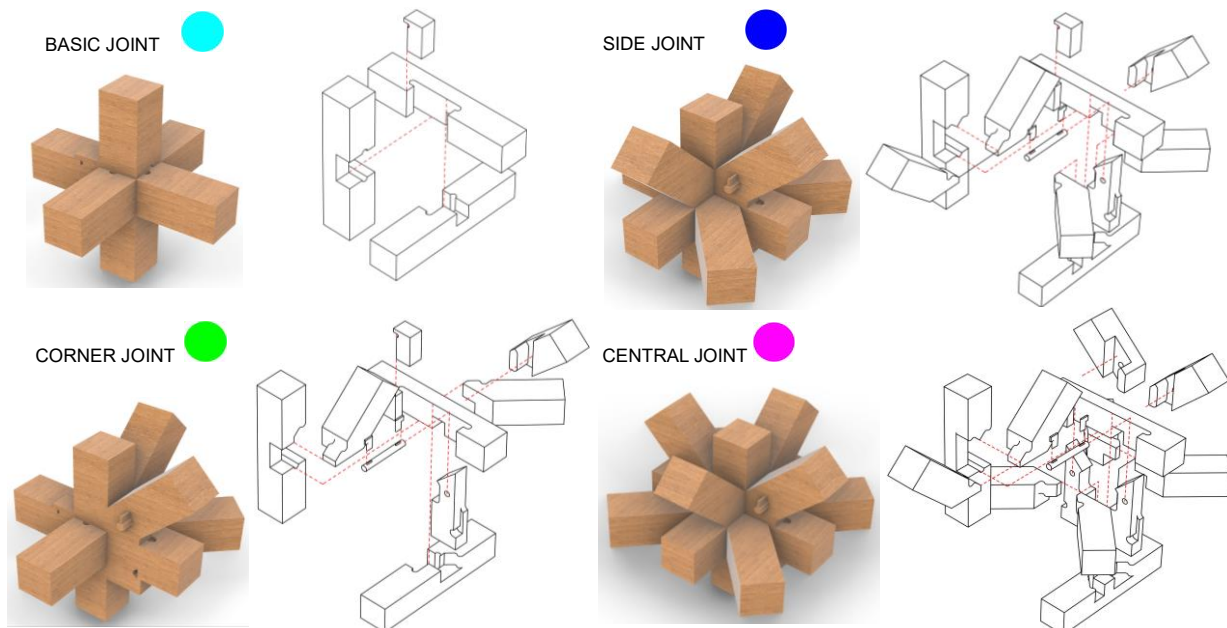


Fig. 19. Adaptations of the “Spatial Masterkey” joining system between node connectors in the “spaceframe module”.

The spatial module to be built using the adaptations of the “complete” node connectors of the “Spatial Masterkey” wood-wood joining system (**Fig. 19 and 20**), will be limited to a flexible spaceframe module that can be dismantled, formed of small -50x50mm- pieces arranged in a cubic, orthogonal, spatial grid of 800x800x800 mm repeated 6 times in the direction of the X and Y axes and once in direction of the Z axis. The grid is complemented by diagonal struts in the 3 directions of the spaceframe, in order to secure the assembly and to prevent the displacement of node connectors and struts (seeking the concentration of the diagonal vertices within a minimum number of nodes, as doing so facilitates the optimization of the resultant nodes).

It is a coplanar spaceframe composed of rectangular prisms with simple struts on all faces of the prisms (active load-bearing vector structural system) [47].

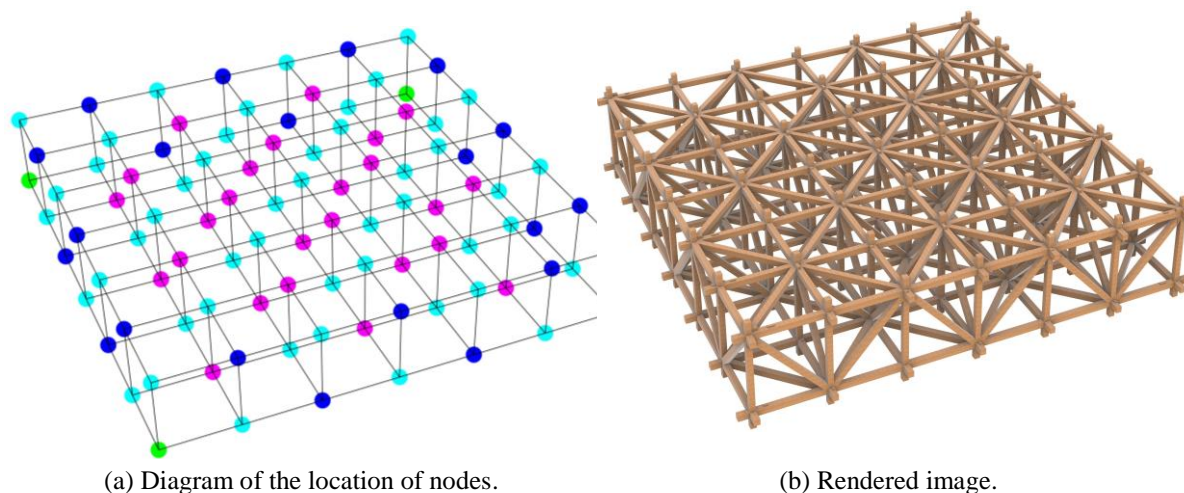


Fig. 20. “Spaceframe module”.

6.2 Evaluation of the stress/strain levels in the struts that form the structural spaceframe module

The software used to calculate the stress on the struts was Dlubal REFM 6 [48].

The criterion considered in Section 4 of this paper was followed when modeling the structural spaceframe module in which the “Spatial Masterkey” joining system was developed, i.e., the forces acting upon the structure will be applied to the nodes.

This hypothesis was corroborated after completing analytical tests of the stress state of the struts with the software program [48]. So, regardless of the connections at the end of the struts -articulated and embedded joints-, the loads applied to the nodes meant that the moments that appeared could be considered insignificant (at least 100 times less than the stress due to axial forces -in the range of 0.01 kNm-). In that respect, it may be indicated that a value of 1 as the coefficient of rigidity of the joint was introduced in the software program, considering that the nodes that formed the spaceframe were articulated.

The considerations taken into account in the calculation of the stresses on the struts that formed the spaceframe module were as follows:

- Select the location of the structure to assign it one of the service classes as a function of the envisaged environmental conditions (art. 2.2.2.2 [1g]). Service class 2 was chosen, considering it to be a covered wooden structure, but with the possibility of being opened and exposed to the exterior.
- Select the wood for its construction. Given the heterogeneous nature of this material, the choice of one type or another implies choosing a strength class (Annex C, Table C.1 [1b]), which will influence the load-bearing capacity (Annex E Table E.1 (3)) of the struts that form the structure. In this case, a sawn wood, *Pinus sylvestris* L. (Spain) was chosen, as mentioned in Section 3 of this paper.
- Evaluate the loads in accordance with current regulations [49] and transfer them to the nodes. These actions -permanent (dead load of the wooden structure) and variable (live load:

0.4kN/m² uniform load and 1kN of occasional load, snow: 0.4kN/m² load, and wind: 0.52kN/m² dynamic pressure- must be grouped into simple hypotheses that will then be combined with the corresponding coefficients, to form the combinations (art. 4.2.2 [50a]) of the Ultimate Limit State (ULS) (art. 3.2.1 [50a]), thereby yielding the calculated axial stress/strain levels. In that respect:

- The actions of an earthquake (art. 1.2.3. [51]), the basic seismic acceleration -a_b- being less than 0.04g.
- Live load was not considered among the other variable actions (Table 3.1[49]).
- It was considered that the structure could support a lightweight roof of 0.46kN/m².

The following graphs (**Fig. 21**) only show the struts of the spaceframe with strain levels above those tested in the physical tests performed on the corresponding struts (specifically some of the diagonal struts subjected to axial traction).

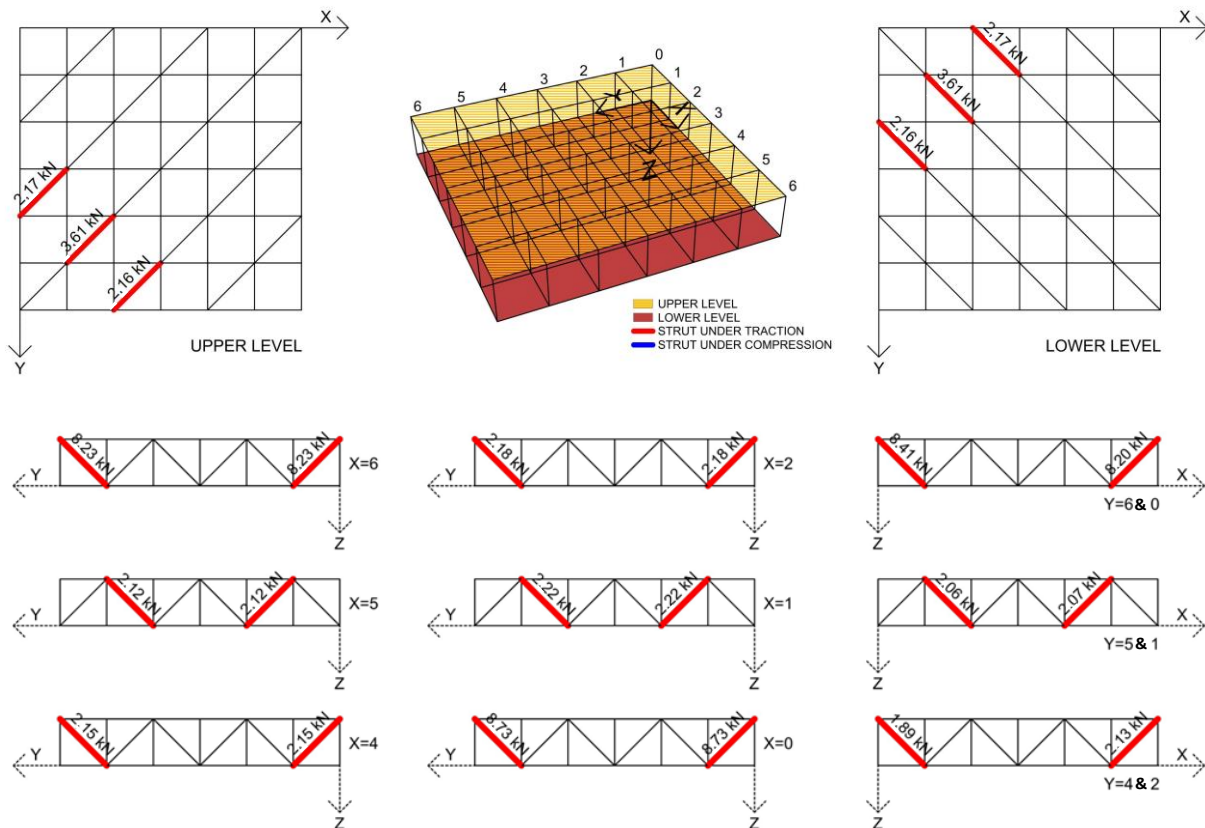


Fig. 21. Struts with strain levels above those evaluated in the physical tests.

It may also be recalled that the sections in use (both of the -50x50 mm- struts and the -8 mm diameter- dowel pins and, consequently, the complementary parts of the nodes), even though quite reduced, yielded results that satisfied the load-bearing requirements of most of the struts that formed the structural spaceframe (all the struts subjected to compression and most of the struts subjected to traction). An interesting piece of information is that the total length of the struts that formed the spaceframe module was, approximately, 280 meters; such that the volume of wood employed for a 50x50 mm section was 0.70 m³.

In that respect, there was no doubt that the use of larger struts with larger effective sections, in which reinforcing dowel pins of a larger diameter could, were it necessary, be inserted, would notably improve the structural performance of the aforementioned struts. It would not only contribute greater load-bearing capacity, but would yield better results than smaller sized struts, given that the impact on the reduction of the effective section -due to the holes that have to be drilled in the struts for the insertion of the aforementioned dowel pins- is less than in the smaller sized struts.

7 Proposed uses for the “Spatial Masterkey” wood-wood joining system

Given that the effective section of the constituent parts of the “Spatial Masterkey” joining system and its adaptations is considerably smaller as a consequence of the machining of each node connector for the assembly of the joint, that sort of joint will therefore have a lower load-bearing capacity. It was therefore concluded, in view of the laboratory test results, that the type of use of the aforementioned node could be valid in structural joints with active load-bearing vectors [47] and low stress levels-loads applied to the nodes- and medium spans, such as façades and non-transitable roofs.

8 Conclusions

Digital manufacturing in architecture has led to the revival of carpentry joints, assembly techniques that fell into disuse as a result of the use of metal fasteners to join pieces together. The industrialization and the mass customization of these traditional joining techniques can now be achieved with CAD/CAM technology applied to wood, making their use highly competitive (speed of machining complex geometries, greater cutting precision and uniformity in the products produced) and environmentally friendly, in so far as the use of metal in the joints is avoided.

Based on this technology, a spatial wood-wood joining system called “Spatial Masterkey” [17] has been developed, with the added bonus that its design and manufacture are adapted to the production parameters of a 3-axis CNC milling machine, with the sole purpose of “democratizing” the manufacturing of the parts that make up this joining system. This type of machine is very simple, low cost and easy to handle, which means that it can be widely used for many applications.

In this paper, the development in terms of design and manufacturing of the “Spatial Masterkey” joining system has been completed, by evaluating its strength capacity through experimental tests at laboratory scale.

A structural calculation was performed based on the “Spatial Masterkey” joining system to obtain the stresses of the bars in a lightweight roof solution, accessible for maintenance work, and the results were compared with the results of the tests on the bar joints. As those joints form a lattice with loads applied at the nodes, they only work under axial tensile and compression stresses.

The results of the experimental tests on the horizontal/vertical bar node, both under tension and compression, yielded satisfactory results with stress values higher than 8.50 kN before failure. As for the tests on the diagonal bars, the compression tests also showed a favorable result with values of the stresses close to 8.00 kN; on the other hand, the tensile tests presented low results at 0.734 kN, because, when tensile stresses run parallel to the fibers, some bars break, as shown in certain graphs.

The use of doweling was proposed to avoid joint failure, which improved the resistant capacity of the pieces by 128%, although that value was still below the necessary values. Hence, the proposal to analyze other improvement options as a future line of research, such as the use of larger sections, and other materials.

The small size of the bars must be taken into account, with sections of 50x50 mm; although, with the exception of the tensile diagonals, all the other pieces met the requirements established in the Spanish Technical Building Code for lightweight roof solutions.

Based on the above, it was estimated that the range of use of the “Spatial Masterkey” joining system with very small sections was suitable for structural solutions with low loads, and loads applied at nodes and medium spans, such as non-transitable façades and roofs.

9 Future line of investigation

As future lines of research, optimization strategies will be proposed to improve the capability of the “Spatial Masterkey” joining system to withstand axial forces -especially traction- the use of larger sections of struts and dowels, as well as the use of wood products, such as plywood -consisting of a board with an odd number of glued sheets arranged so that the fiber of one sheet is perpendicular to the next. It is characterized as a material with similar mechanical properties in all directions of the plane of the board [52]-, whose resistance to axial forces is greater than that of sawn wood precisely because of

the arrangement of the plywood sheets that limits any stress-related breakages due to low resistance (shear parallel to the fiber and traction perpendicular to the fiber).

Acknowledgments

The authors are grateful to the technicians of Fablab Donostia for their collaboration in the manufacture of the parts that appear in the photographs of this paper. They would also like to acknowledge the SAREN research group (IT1619-22, Basque Government) for the translation of this article.

Funding Statement

The authors received no specific funding for this study.

CRedit authorship contribution statement

Antonio Jesús de-los-Aires-Sol í: Conceptualization, Investigation, Methodology, Formal analysis, Writing – original draft, Writing – review & editing. **Jesús Cuadrado Rojo:** Resources, Supervision, Review & Editing.

Conflicts of Interest

The authors declare that they have no conflicts of interest to report regarding the present study.

References

- [1] DB SE-M. Documento Básico Seguridad Estructural-Madera, Código Técnico la Edificación, Ministerio de Fomento, Gobierno de España, 2019; [1a] Art. 5.2: 23, [1b] App. C. Table C.1: 111, [1c] App. E. Table E.1: 115, [1d] Art. 6.1.8: 31, [1e] Art. 6.1.3: 29, [1f] Art. 6.2.3: 33, [1g] Art. 2.2.2.2: 11. <https://www.codigotecnico.org/pdf/Documentos/SE/DBSE-M.pdf>.
- [2] Cueva C, La fabricación digital y su aplicación en el ámbito de la educación superior universitaria: el laboratorio de fabricación digital FabLab, Universidad San Pablo CEU, Madrid, 2017. <http://hdl.handle.net/10637/8436>.
- [3] Ferrer Franco P, Fabricación digital en la arquitectura. La transformación de los procesos de proyecto, Final Degree Project, 2015. <https://aula3tfg.wordpress.com/wp-content/uploads/2016/02/tfg-pablo-final.pdf>.
- [4] Argüelles Alvarez R, Uniones: un reto para construir con madera: discurso del académico leído en la sesión inaugural del año académico el día 26 de enero de 2010, Real Academia de Ingeniería, Madrid, 2010. <https://www.caminoCastillaLeon.es/wp-content/uploads/Ingenieria-Humanismo/Ramon%20Arguelles%20Leccion%202010%20RAI.pdf>
- [5] Graubner W, Ensamblados en madera. Soluciones japonesas y europeas, Ceac, Barcelona, 1991; 19.
- [6] Erman E. Timber joint design: the geometric breakdown method. *Building Research & Information* 2002; 30(6): 446-469. <https://doi.org/10.1080/09613210210150991>.
- [7] D. Jiménez Gutiérrez D, Constructividad de las uniones carpinteras fabricadas digitalmente para la edificación en mediana altura, Universidad de Chile, 2021. <https://repositorio.uchile.cl/handle/2250/199173>.
- [8] González Böhme L, Maino Ansaldo S, Uniones carpinteras de Valparaíso: La geometría de ensambles y empalmes, RiL editores, 2019.
- [9] Carpo M, The alphabet and the algorithm, Mit Press, Cambridge, Massachusetts, 2011.
- [10] Davis S, Future Perfect, Addison Wesley Publishing Company, Reading, Massachusetts, 1987.
- [11] Camille Halabi M, Los inicios de la aplicación de la tecnología CAM en la arquitectura: la Sagrada Familia, Doctoral Dissertation, Universitat Internacional de Catalunya. Departament d'Arquitectura, 2008. <http://hdl.handle.net/10803/9330>.
- [12] Pine J, Mass Customization: The New Frontier in Business Competition, Harvard Business School Press, Boston, Massachusetts, 1992; 131-170.
- [13] Zellner P, Hybrid Space: New forms in Digital Architecture, Thames and Hudson, 1999; 12.
- [14] Informe de Indicadores de Sostenibilidad 2023. Desempeño de la industria siderúrgica en materia de sostenibilidad 2004-2022. <https://worldsteel.org/steel-topics/sustainability/sustainability-indicators-2023-report/>, 2024 (accessed 15 September 2024).
- [15] La huella del carbono en el sector del acero. <https://irp.cdn-website.com/acef31c6/files/uploaded/Huelladecarbonoenelsectoracero.pdf>, 2022 (accessed 15 September 2024).
- [16] Acero sostenible: ¿qué tiene que ver el cambio climático con el acero? <https://climatescience.org/es/advanc>

- ed-steel-climate, 2024 (accessed 15 September 2024).
- [17] de-los-Aires-Solis AJ, Gonzalez-Quintal F. A wood-wood joining system suitable for digital fabrication and its application in the design of a “wood-only” spatial module, *Frontiers of Architectural Research* 2023; 12(3): 523-540. <https://doi.org/10.1016/j.foar.2022.12.005>.
- [18] Gamarro J, Bocquet JF, Weinand Y. Experimental investigations on the load-carrying capacity of digitally produced wood-wood connections. *Engineering Structures* 2020; 213: 110576. <https://doi.org/10.1016/j.engstruct.2020.110576>.
- [19] Beneficios Madera – Forestales Latinoamericanos. <https://forestaleslatinoamericanos.com/beneficios-madera/>, 2024 (accessed 15 September 2024).
- [20] Marcos Martín F, Ruiz Castellano J, Izquierdo Osado MI. La madera como fijadora de CO₂. *Boletín de Información Técnica. AITIM* 2001; 210: 63-67. https://infomadera.net/uploads/articulos/archivo_4108_12258.pdf.
- [21] Rojo-Martínez GE, Jasso-Mata J, Velásquez-Martínez A. Las masas forestales como sumideros de CO₂ ante un cambio climático global. *Revista Chapingo. Serie Ciencias Forestales y del Ambiente*. 2003; 9(1): 57- 67. <https://www.redalyc.org/pdf/629/62990106.pdf>.
- [22] Gershenfeld N, FAB. *The Coming Revolution on your Desktop*, Basic Books, Nueva York, 2005.
- [23] Peek N, *Making machines that make: object-oriented hardware meets object-oriented software*, PhD thesis, Massachusetts Institute of Technology, 2016. <https://dspace.mit.edu/handle/1721.1/107578>.
- [24] UNE 56544, *Visual grading for structural sawn timber. Coniferous timber*, 2022.
- [25] Fang D, Moradei J, Brütting J, Fischer A, Landez DK, Shao B, Sherrow-Groves N, Fivet C, Mueller C, Modern timber design approaches for traditional Japanese architecture: analytical, experimental, and numerical approaches for the Nuki joint, In *Proceedings of IASS Annual Symposia, Barcelona, International Association for Shell and Spatial Structures (IASS)*, 2019. <https://infoscience.epfl.ch/server/api/core/bitstreams/7098fd91-1f31-4e32-8558-19965355fbc8/content>.
- [26] Fang D, Mueller C, Joinery connections in timber frames: analytical and experimental explorations of structural behavior, In *Proceedings of IASS Annual Symposia, Boston, International Association for Shell and Spatial Structures (IASS)*, 2018. https://www.researchgate.net/profile/Demi-Fang/publication/326674720_Joinery_connections_in_timber_frames_analytical_and_experimental_explorations_of_structural_behavior/links/5b5d253caca272a2d672774d/Joinery-connections-in-timber-frames-analytical-and-experimental-explorations-of-structural-behavior.pdf.
- [27] [20_Joinery_connections_in_timber_frames_analytical_and_experimental_explorations_of_structural_behavior/links/5b5d253caca272a2d672774d/Joinery-connections-in-timber-frames-analytical-and-experimental-explorations-of-structural-behavior.pdf](https://www.researchgate.net/profile/Demi-Fang/publication/326674720_Joinery_connections_in_timber_frames_analytical_and_experimental_explorations_of_structural_behavior/links/5b5d253caca272a2d672774d/Joinery-connections-in-timber-frames-analytical-and-experimental-explorations-of-structural-behavior.pdf).
- [28] Moradei J, Brütting J, Fivet C, Sherrow-Groves N, Wilson D, Fischer A, Ye J, Cañada J, Structural characterization of traditional moment-resisting timber joinery, In *Proceedings of IASS Annual Symposia, Boston, International Association for Shell and Spatial Structures (IASS)*, 2018. <https://infoscience.epfl.ch/server/api/core/bitstreams/a74c9a2c-9c67-48b2-9da2-655513eaff33/content>.
- [29] Fang DL, Mueller CT, Brütting J, Fivet C, Moradei J, Rotational stiffness in timber joinery connections: Analytical and experimental characterizations of the Nuki joint, *Structures and Architecture: Bridging the Gap and Crossing Borders, Proceedings of the 4th International Conference on Structures and Architecture, ICSA*, 2019. <https://dspace.mit.edu/bitstream/handle/1721.1/137072/fullpaper.pdf?sequence=2&isAllowed=y>.
- [30] ¿Método numérico, analítico y experimental: concurrentes o complementarios en la ingeniería? <https://www.esss.com/es/blog/simulacion-numerica-metodos-analitico-experimental-concurrentes-o-complementarios-en-la-ingenieria/>, 2017 (accessed 2 July 2024).
- [31] Judd JP, Fonseca FS, Walker CR, Thorley PR. Tensile strength of varied-angle mortise and tenon connections in timber frames. *Journal of Structural Engineering* 2012; 138(5): 636-644. [https://doi.org/10.1061/\(ASCE\)ST.1943-541X.0000468](https://doi.org/10.1061/(ASCE)ST.1943-541X.0000468).
- [32] Koch H, Eisenhut L, Seim W. Multi-mode failure of form-fitting timber connections—Experimental and numerical studies on the tapered tenon joint. *Engineering Structures* 2013; 48: 727-738. <https://doi.org/10.1016/j.engstruct.2012.12.002>.
- [33] Panoutsopoulou L, Mouzakis C. Experimental investigation of the behavior of traditional timber mortise-tenon T-joints under monotonic and cyclic loading. *Construction and Building Materials* 2022; 348: 128655. <https://doi.org/10.1016/j.conbuildmat.2022.128655>.
- [34] Chen Z, Zhu E, Lam F, Pan J. Structural performance of Dou-Gong brackets of Yingxian Wood Pagoda under vertical load—An experimental study. *Engineering Structures* 2014; 80: 274-288. <https://doi.org/10.1016/j.engstruct.2014.09.013>.
- [35] Tannert T, Lam F, Vallée T. Structural performance of rounded dovetail connections: experimental and numerical investigations. *European Journal of Wood and Wood Products* 2011; 69: 471-482. https://doc.rero.ch/record/317927/files/107_2010_Article_459.pdf.
- [36] Steiniger M, Strength and performance of the INDUO®-heavy-timber connector in combination with structural composite lumber and Douglas-Fir, Doctoral Dissertation, Dept. of Wood Sci., Univ. of British Columbia, 2003. <http://hdl.handle.net/2429/14327>.

- [37] Garbin E, Valluzzi MR, Modena C, Characterization of a dovetail joint for timber roofs, In World Conference on Timber Engineering, 2006. <https://www.research.unipd.it/handle/11577/2442118>.
- [38] Tannert T, Structural performance of rounded dovetail connections, Doctoral dissertation, University of British Columbia, 2008. <http://hdl.handle.net/2429/694>.
- [39] Pang SJ, Oh JK, Park CY, Lee JJ, Effects of Size Ratios on Dovetail Joints in Korean Traditional Wooden Building, In World Conference on Timber Engineering, 2012. <https://www.diva-portal.org/smash/get/diva2:1003786/FULLTEXT02.pdf>.
- [40] Sangree RH, Schafer BW. Experimental and numerical analysis of a stop-splayed traditional timber scarf joint with key. *Construction and Building Materials* 2009; 23(1): 376-385. <https://doi.org/10.1016/j.conbuildmat.2007.11.004>.
- [41] Massaro FM, Stamatopoulos H, Andersen J, Brekke-Rasmussen E. Finite element modelling and experimental verification of timber halved and tabled scarf joints. *International Wood Products Journal* 2023; 14(1): 3-12. <https://journals.sagepub.com/doi/pdf/10.1080/20426445.2022.2133469>.
- [42] Aira Zunzunegui JR, Análisis experimental y por el método de los elementos finitos del estado de tensiones en uniones carpinteras de empalme de llave, Doctoral Dissertation, Universidad Politécnica de Madrid. Escuela Técnica Superior de Ingenieros de Montes, 2013. https://oa.upm.es/21832/1/JOSE_RAMON_AIRA_ZUNZUNEGUI.pdf.
- [43] Aira JR, Arriaga F, Iñiguez-González G, Guaita M. Failure modes in halved and tabled tenoned timber scarf joint by tension test. *Construction and Building materials* 2015; 96: 360-367. <https://doi.org/10.1016/j.conbuildmat.2015.08.107>.
- [44] Sangree RH, Schafer BW. Experimental and numerical analysis of a halved and tabled traditional timber scarf joint. *Construction and Building Materials* 2009; 23: 615-624. <https://doi.org/10.1016/j.conbuildmat.2008.01.015>.
- [45] Palma P, Ferreira J, Cruz H, Monotonic tests of structural carpentry joints, In World Conference on Timber Engineering, 2010. https://www.researchgate.net/profile/Joao-Gomes-Ferreira/publication/289578855_Monotonic_tests_of_structural_carpentry_joints/links/5e67d28392851c7ce05aea09/Monotonic-tests-of-structural-carpentry-joints.pdf.
- [46] Villar-García JR, Vidal-López P, Crespo J, Guaita M, Analysis of the stress state at the double-step joint in heavy timber structures. *Materiales de construcción* 2019; 69(335). <https://doi.org/10.3989/mc.2019.00319>.
- [47] Feio AO, Lourenço PB, Machado JS. Testing and modeling of a traditional timber mortise and tenon joint. *Materials and structures* 2014; 47: 213-225. <https://repositorio.inec.pt/bitstream/123456789/1006075/1/Arquivo%202023%20Feio%20Lourenco%20and%20Machado%20Materials%20and%20Structures%202014.pdf>.
- [48] Engel H, *Sistemas de estructuras. Sistemas estruturais*, Editorial Gustavo Gili S.L, Barcelona, 2006; 157.
- [49] REFM 6. Version 6.02.0050. Dlubal Software.
- [50] DB SE-AE. Documento Básico Seguridad Estructural-Acciones en la Edificación, Código Técnico la Edificación, Ministerio de Fomento, Gobierno de España, 2009. <https://www.codigotecnico.org/pdf/Documentos/SE/DBSE.pdf>.
- [51] DB SE. Documento Básico Seguridad estructural, Código Técnico la Edificación, Ministerio de Fomento. Gobierno de España, 2019; [50a] art. 4.2.2: 15-16, [50b] art. 3.2.1: 11. <https://www.codigotecnico.org/pdf/Documentos/SE/DBSE.pdf>.
- [52] Norma de Construcción Sismorresistente. Parte general y edificación (NCSE-02), Ministerio de Fomento. Gobierno de España, 2002. https://www.transportes.gob.es/recursos_mfom/0820200.pdf.
- [53] Arriaga Martitegui F, *Estructuras de madera*, Revista Tectónica. Monografías de arquitectura, tecnología y construcción 13. Madera (II). Estructuras, ATC Ediciones S.L, 2001; 10
- [54] WikiHouse. <https://www.wikihouse.cc/> (accessed 20 October 2024).
- [55] Boano Prišmontas. The Arches Project. <https://www.boanoprismontas.com/thearchesproject> (accessed 20 October 2024).
- [56] Xframe. <https://xframe.com.au/> (accessed 20 October 2024).
- [57] CLICK-RAFT. <https://click-raft.blogspot.com/> (accessed 20 October 2024).
- [58] Sass L, A wood frame grammar: A generative system for digital fabrication, *International Journal of Architectural Computing* 2006; 4:51-67. <https://doi.org/10.1260/147807706777008920>.
- [59] Albright D, Blouin V, Harding D, Heine U, Huette N, Pastre D, Sim[ply]: Sustainable construction with prefabricated plywood componentry, *Procedia environmental sciences* 2017; 38: 760-764. <https://doi.org/10.1016/j.proenv.2017.03.159>
- [60] [SI-MODULAR]®. <https://www.si-modular.net/> (accessed 20 October 2024).